Protection of electronics from environmental temperature spikes by phase change materials

M. E. Kiziroglou* and E. M. Yeatman

Electrical and Electronic Engineering Department
Imperial College London
London SW7 2AZ, United Kingdom

*Corresponding Author: m.kiziroglou@imperial.ac.uk

Abstract

Protection of electronics from high temperature environments is desirable in applications such as harsh environment industrial sensor networks for continuous monitoring and probing. In this paper, the use of phase-change-material (PCM) encapsulation of electronics is proposed as protection from environment-induced, probing-induced or electronic power burst - induced temperature spikes. An outline of the encapsulation method is given and a heat flow analysis is performed. A lumped element model is introduced and a numerical simulator is implemented. An encapsulation setup is fabricated and tested, allowing an experimental validation of the proposed method and model. The numerical simulation model is then used to study particular temperature spike scenarios. The results demonstrate that at reasonable encapsulation sizes and for commercially available phase-change and insulation materials, short-term protection from large temperature spikes can be provided by the proposed method. As an indicative example, for a typical sensor node normally operating at a 20 ^{o}C environment, PCM encapsulation may provide protection for 28 s of exposure to 1000 ^{o}C per PCM gram.

Keywords: phase change materials, harsh environment, electronics, transient

I. INTRODUCTION

In recent years, the combination of heat sinking structures with phase change materials (PCMs) has been proposed and studied, as cooling structures for electronics that are not operated continuously [1]. Three dimensional simulation modeling and experimental studies have been reported, revealing the benefits of PCM solutions [2, 3]. Various applications have been studied such as portable electronics [4], photovoltaic thermal management [5], heat sinking for cameras carried by fire fighters [6] and high energy batteries including implementations for vehicles [7-9]. Reviews of the application of PCMs in thermal management of electronics can be found in the literature [10, 11]. The reported systems typically involve management of the heat dissipation of electronics, specifically for systems with intermittent activity such as wireless sensors.

In this paper, a PCM encapsulation solution is proposed and assessed for harsh environment applications, where transient high temperatures occur. Such applications include probe measurement systems and industrial monitoring of systems involving a time-cycled heat operation. A simple analytical approach is introduced, including a numerical model. This model is validated experimentally and used to perform a quantitative study of the protection that can be provided by PCMs, assessing the performance of different material and geometrical parameters.

II. SYSTEM CONCEPT

An electronic device is encapsulated in a phase change material (PCM) of heat capacity C and latent heat L, with phase change at T_{PCM} as illustrated in Figure 1. The temperature of the electronic device is T_D. The PCM is insulated from the environmental temperature T_{OUT} by an insulation layer of thermal resistance R. During operation, the device dissipates power at a constant rate P. It is assumed

Published as: Kiziroglou and Yeatman, Journal of Electronic Materials, 44, 4589-4594, 2015

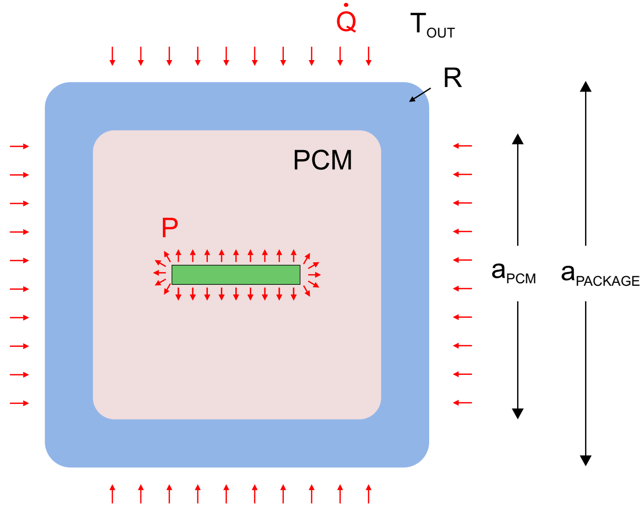

Fig. 1 Conceptual schematic of a PCM encapsulated device

that the PCM temperature T_{PCM} is uniform and equal to T_D, i.e. the PCM thermal resistance is very small in comparison to R. It is also assumed that no significant heat radiation occurs and that the only material of significant heat capacity is the PCM. Under these assumptions, the heat dynamics of the system can be studied with reference to the lumped element model presented in Figure 2.

III. ANALYTICAL AND NUMERICAL MODEL

During non-phase change operation, the heat flow dynamics of the system are governed by the following equations:

$$Q_{PCM} = C \cdot T_D \tag{1}$$

$$\dot{Q} = \frac{T_{OUT} - T_D}{R} \tag{2}$$

$$\dot{Q}_{PCM} = \dot{Q} + P \tag{3}$$

where Q_{PCM} is the sensible heat energy stored in the PCM, $\dot{Q}$ is the heat flow through R and $\dot{Q}_{PCM}$ is the heat flow into the PCM. By simple combination of these equations, the non-phase change differential equation of the system can be derived, giving:

$$\tau \dot{T}_D + T_D = T_{OUT} + RP \tag{4}$$

where $\tau = RC$ is the system time constant. The analytical solution of this equation depends on the time variation of T_{OUT} and P. When the latter are constant, T_D reaches steady-state, at an equilibrium value of:

$$T_{D,steady-state} = T_{OUT} + RP \tag{5}$$

If either T_{OUT} or P change abruptly to a new constant value, T_D reaches the new steady-state exponentially with time constant τ. During phase change, equation (1) is not valid as T_D remains constant until all latent heat is exchanged. In order to study the system in the general case, including phase change and arbitrarily changing T_{OUT} and P,

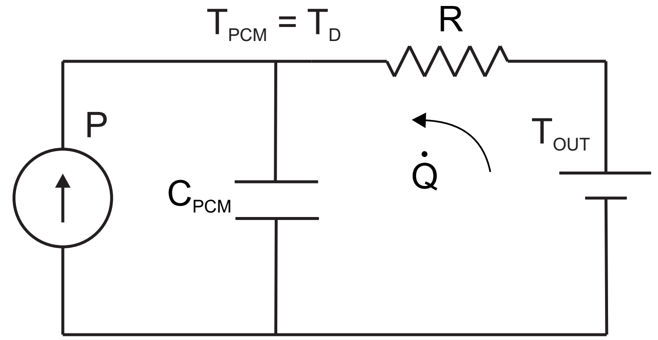

Fig. 2 Lumped element circuit model of a PCM encapsulated device

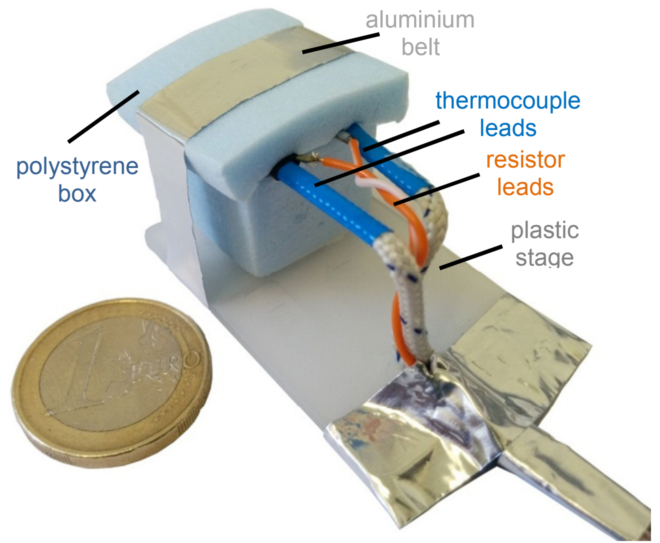

Fig. 3 Photograph of the experimental setup used for model validation.

a numerical model can be formulated based on the above equations. If Δt is the time step between system states [n] and [n+1] and NPC and PC indicate non-phase change and phase change operation respectively, every new state $[T_D(n+1), \dot{Q}_{PCM}(n+1)]$ can be calculated from the previous state $[T_D(n), \dot{Q}_{PCM}(n)]$ and input $[T_{OUT}(n), P(n)]$ as:

$$T_D(n+1) = \begin{cases} T_D(n) + (T_{OUT}(n) - T_D(n) + RP(n)) \cdot \frac{\Delta t}{\tau} & ,NPC \\ T_D(n) & ,\ PC \end{cases} \tag{6}$$

$$Q_{PCM}(n+1) = Q_{PCM}(n) + \left(P(n) + \frac{T_{OUT}(n) - T_D(n)}{R}\right) \cdot \Delta t \tag{7}$$

IV. EXPERIMENTAL VALIDATION

As an experimental assessment of the proposed protection method, a prototype PCM encapsulation module was built and tested for environmental temperatures up to 90 ^{o}C. An image of this module is presented in Figure 3.

Published as: Kiziroglou and Yeatman, Journal of Electronic Materials, 44, 4589-4594, 2015

The encapsulation is cubic, with external and internal side length of 20 mm and 15 mm respectively and includes 3 cm^3 of a paraffin based PCM with phase change at 60 ^oC, 100 J/g latent heat, heat capacity of 2 kJ / kg K, heat conductivity of 0.25 W/mK and density 900 kg/m^3. This PCM volume allows around 10% of additional space to account for the thermal expansion that is expected in the temperature range of the experiment, in particular 20 ^oC – 110 ^oC. The insulation layer is made of 2.5 mm thick extruded polystyrene with a heat conductivity of 0.03 W/mK. The device under protection was emulated by a 120 Ω resistor, supplied with a DC voltage of 5 V and dissipating around 200 mW during experiments. The resistor was suspended at the centre of the PCM material using its own wires for mechanical support. A thermocouple was placed by the resistor to monitor its temperature, and a second one was placed by the inner surface of the insulation to monitor the interior temperature gradient.

The response of this setup when exposed to different environmental temperatures was recorded, with a temperature upper limit of 90 ^oC, in order to avoid any thermal damage on the polystyrene insulation. A characteristic temperature response is presented in Figure 4. Initially, the device was at steady state, at a room temperature of 24 ^oC, with no power applied to the resistor. At t = 0 min, the resistor was supplied with 200 mW, driving the device temperature T_D to a new steady state of 35 ^oC, after around 20 min. At t = 22 min, the setup is immersed into an oven, heated at 90 ^oC. At this point, as expected by equation (5), T_D increased towards a new steady state of T_{OUT} + RP. When it reached the range of the PCM melting point, this increase was slowed down, until the phase change was completed. The duration of the phase change was 10 min. Subsequently, T_D continued its increase up to 100 ^oC, where it stabilized at t = 43 min. At t = 45 min, the setup was put back to the 24 ^oC room environment. The device temperature was reduced towards the new steady state (again 35 ^oC, since the power dissipation on the resistor continues), until solidification begins, at around 50 ^oC. After completion of the phase change, T_D continued to decrease towards 35 ^oC. At t = 69 min the resistor power was turned off, allowing the setup to return to its passive steady state at 24 ^oC.

The temperature difference within the PCM, monitored using the second thermocouple at the inner surface of the insulation, was in the range of a few ^oC throughout the experiment, indicating a finite PCM thermal conductivity. This temperature gradient is small in comparison to the overall temperature range and doesn't affect the discussion of this section. The implications of PCM thermal conductivity to performance are further discussed in section V.

In order to compare this experimental response with the analysis of the previous section, a simulation of the device response, based on equations (6) and (7) is also plotted in Figure 4.

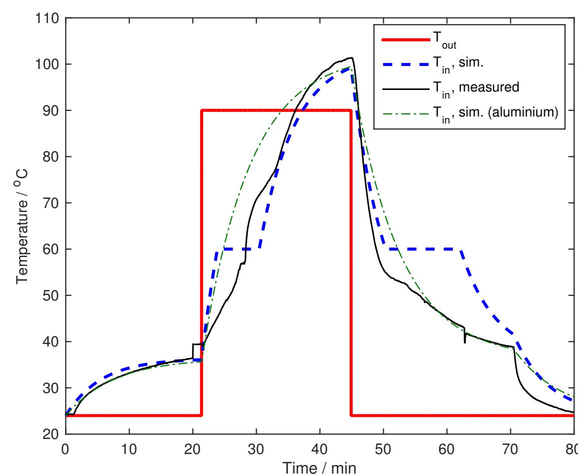

Fig. 4 Measured thermal response of the setup shown in Fig. 3, at 200 mW encapsulated device power and a 23 min, 90 ^oC thermal pulse. The corresponding simulated response based on equations (6) and (7) for the parameters of the PCM used and also for an aluminium encapsulation case with the same size and insulation are also shown for comparison.

For this simulation, the nominal values of C, R and P from the experimental conditions were used, for the case of a PCM material with the same property values as given for the experiment. The experimental and simulated data show significant similarity, validating the proposed simulation method and allowing its use in the prediction of response for different device designs and environmental conditions.

The same simulation was run for the case of using aluminium as a non-phase change high specific heat capacity material, with all the other specifications (geometry, dimensions, insulation properties, device power consumption and environmental conditions) kept the same. The corresponding response is plotted as a dash-dotted curve in Figure 4. The comparison between the PCM and the aluminium results demonstrate that a significant delay is obtained by the use of PCM, in the range between 2 and 5 minutes depending on the temperature tolerance limit. In this particular experimental test, the small temperature spike that was applied and the low quality of the PCM that was used resulted in a rather moderate difference between the aluminium and the PCM cases. This performance can be significantly improved by employing PCMs of higher latent heat and specific heat capacity. A simulation study of performance for different encapsulation cases, including an analytical determination of the expected protection time is presented in the next section.

V. SIMULATION OF ENCAPSULATION PERFORMANCE

Based on the analysis of section III, the temperature response for different encapsulation designs and heating scenarios can be simulated, by applying the numerical equations (6) and (7).

Published as: Kiziroglou and Yeatman, Journal of Electronic Materials, 44, 4589-4594, 2015

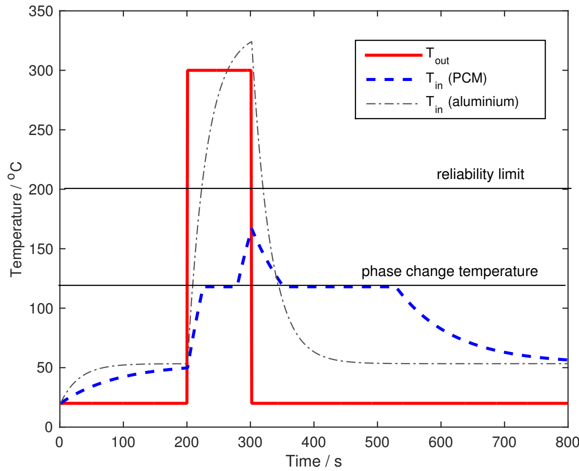

Fig. 5 Simulated thermal response to a 300 °C, 100 s environmental thermal spike, for 1 g of PCM with L = 340 J, C = 2.7 J/K and 2 mm of a 0.1 W/mK insulator giving an R_I = 33.3 K/W. The equivalent response of 1 g of Al and the same insulation is also simulated for comparison.

The main objective of such response simulations is to study and quantify the protection that is provided by PCM encapsulation from temporal environmental temperature peaks but also from internal heat production spikes. Simulation results for a commercially available PCM (A118 from PCM Products Ltd [8]) are shown in Figure 5. The results correspond to 1 g of PCM (total L = 340 J and C = 2.7 J/K) insulated from the environment by a 2 mm, 0.1 W/mK material, yielding an R = 33.3 K/W for the surface of a cubic cm. This insulator thermal conductivity value corresponds to calcium silicate which is typically used in high temperature thermal insulation applications. A chip heat dissipation of P = 1 W is assumed, corresponding to portable electronics applications. A reliable operational temperature limit of 200 °C is assumed [12]. An indicative example for a temperature spike from 20 °C to 300 °C, with a duration of 100 s is studied.

When the device is not operating, the system has an equilibrium state at which T_D and T_{OUT} are both equal to the environmental temperature, 20 °C. At t = 0 the device starts to operate and T_D increases exponentially to 53.3 °C due to the device power dissipation P, with time constant $\tau = RC$, as described by eq. 4. When a T_{OUT} spike occurs, T_D increases, with the same τ, towards its new steady-state, 333 °C (eq. 5). When T_{PC} is reached, the increase pauses as the PCM absorbs the heat flow, up to its latent heat energy L. Then, the exponential temperature increase resumes, until it is again interrupted when the T_{OUT} spike ends. Then, the device temperature decreases exponentially toward 53.3 °C. The decrease is once more interrupted by phase change and eventually the new steady state is reached. The delay in temperature increase that is introduced by the phase change protects the device, keeping it under a certain limit.

For comparison, the equivalent response of an Al encapsulation with the same mass and insulation has also been studied numerically. The specific heat capacity assumed for aluminium is 900 J/kgK.

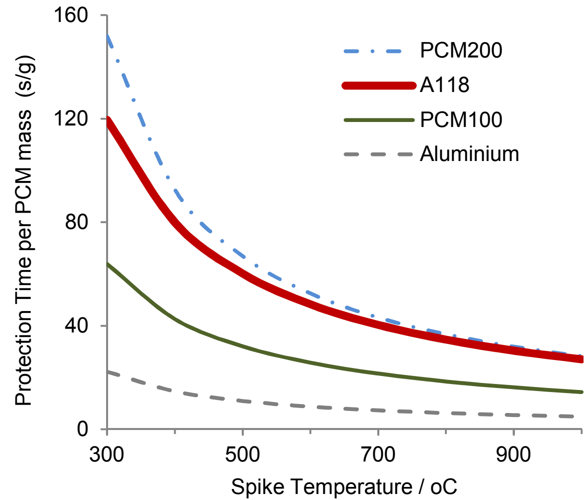

Fig. 6 Protection time vs spike temperature for different PCM materials [13]. Corresponding results for a simple aluminium encapsulation is also shown for comparison

The corresponding response under the same temperature profile conditions is shown as a dash-dotted curve in Figure 5. The response is similar, with an exponential increase and decrease, at a time constant corresponding to the aluminium heat capacity, but without the phase-change effects. This leads to a much faster temperature increase towards the new steady state value. For the particular 100 s temperature spike assumed, the aluminium encapsulation fails to keep the device temperature below the 200 °C reliability limit.

It is possible to calculate the overall protection duration that is provided by a material of given C and L by integration of equation (4) and solution with respect to time. By appropriate setting of integration limits, the time t_P required for a temperature transition from an initial value $T_D(0)$ to the upper limit of reliable operation T_{MAX} can be expressed analytically. By taking phase change also into account (at a temperature T_{PC}), the following equation is derived:

$$t_P = \frac{RL}{T_{OUT}+PR-T_{PC}} + RC \cdot ln\frac{T_{OUT}+PR-T_D(0)}{T_{OUT}+PR-T_{MAX}}$$

The first term in the above equation corresponds to the phase change duration, while the second term corresponds to the time required for the transition from $T_D(0)$ to T_{MAX}. The increase is exponential towards the new steady state value of T_{OUT} + PR. Results of protection time calculation for three different PCMs [13], as a function of peak outside temperature T_{OUT} are shown in Figure 6. The first PCM, denoted as PCM100 was an assumed average performance material with phase change at 100 °C, latent heat 100 J/g and heat capacity 2 J/gK. The second one was the A118 PCM product of PCM Materials Ltd, with phase change at 118 °C, latent heat 340 J/g and heat capacity 2.7 J/gK [13]. The third one, denoted as PCM200, was a material equivalent to the A118 with a phase change at 200 °C. The results presented in Figure 6 correspond to P = 1 W, R = 33.3 K/W, T_{MAX} = 200 °C and a starting environmental temperature of 20 °C.

Published as: Kiziroglou and Yeatman, Journal of Electronic Materials, 44, 4589-4594, 2015

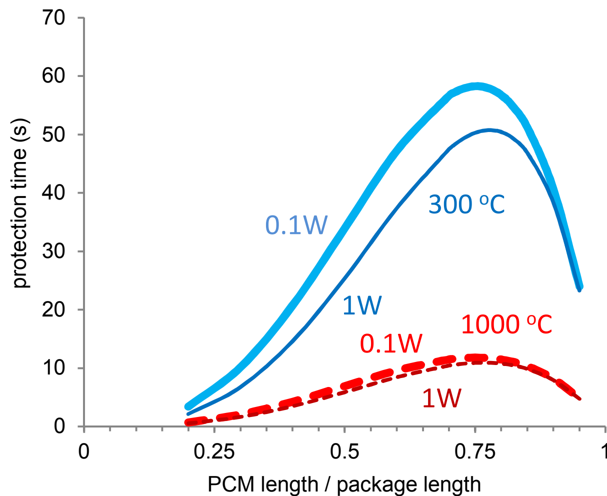

Fig. 7 Numerical calculation of τ_P vs PCM/total length ratio for a 1 cm^3 package, the A118 PCM and a 0.1 W/mK insulator. Results are plotted for two different environmental temperatures and two different device power values

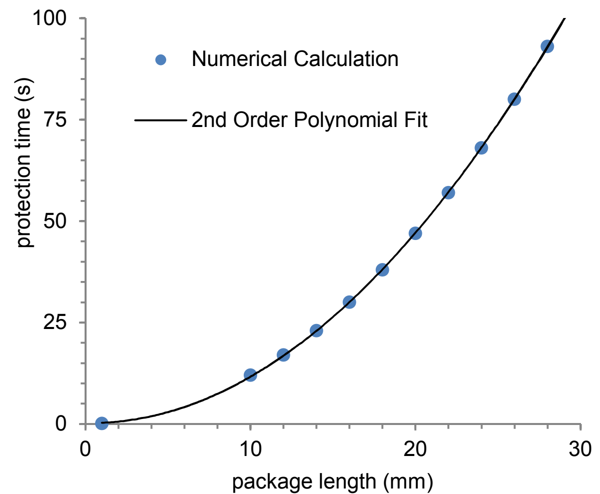

Fig. 8 Scaling of τ_P with package length along with a square fit for P = 0.1 W, T_{out} = 1000 ^{o}C

The results demonstrate protection for 28 s per gram of PCM used from a 1000 ^{o}C environment. This protection time is considerably longer than that achieved by the aluminium encapsulation case (5 s per gram).

Equation (8) can also be used to investigate the effect of the relative size of PCM and insulation to the total protection time for a cubic geometry. Numerical results are plotted in Figure 7 for the A118 PCM. An optimum PCM length percentage of around 75% is observed, corresponding to the maximization of the RL and RC terms. This value can be analytically derived by parametric analysis of equation (8), assuming a low PR term (e.g. 3 K at P = 0.1 W). The scaling of t_P with package length for Tout = 1000 ^{o}C, P = 0.1 W and the A118 PCM are shown in Figure 8. Scaling with the square of side length is observed. This corresponds to the square scaling of the RL and RC terms with package length.

In practice, due to the finite thermal conductivity of PCMs, phase change occurs in a gradual manner across an encapsulation container, resulting in a temperature shift as exhibited by the experimental results of Figure 3. The phase change propagation in the container depends on the PCM properties as well as on the geometry and can be modeled by solution of the Stefan problem. It can affect the protection performance by introducing additional thermal resistance between the device and the environment [14]. In typical PCM thermal management applications, internal heat spreading structures such as fins are employed to suppress this effect, because the objective there is the maximization of heat sinking. In contrast, for protection from environmental heat, a thermal design that maximizes t_p must be sought, taking into account internal PCM temperature gradients and phase-change inhomogeneity. In this direction, the proposed model could be applied in combination with the analysis presented in [14] for the design of optimal fin structures, including multi-cavity PCM container geometries [6, 15].

In the experimental results, the thermal conductivity ratio for the polystyrene insulation and the paraffin PCM used is around one order of magnitude. Therefore, the PCM thermal conductivity is increasing the total thermal resistance. This in turn increases the protection time between the device and the environment, by a small amount. In a practical encapsulation product, a high temperature insulator such as calcium silicate with thermal conductivity around 0.1 W/mK could be used. This is only two times smaller than commercial organic PCMs and five times smaller than hydrated salt based PCMs. Overall, the assumption of a zero thermal resistance by the model, in addition to phase change inhomogeneity, results in an under-estimation of the protection time. Hence, during non-phase change operation, any significant thermal resistance of the PCM should be taken into account as an increase of the total R of the system.

VI. CONCLUSION

The introduction of PCM packaging for protection of electronics from transient high temperatures has been proposed. An analytical and a numerical model have been developed and validated against experimental results, allowing a quantitative study on the protection duration for various cases. Indicatively, state-of-the-art PCMs are expected to provide protection for 28 s per gram at 1000 ^{o}C. A parametric analysis has revealed that in a cubic packaging, the optimum PCM side length a_{PCM} is 75% of the total package side length $a_{PACKAGE}$, achieving the maximum values for RL and RC. The protection time scales with the square of the total packaging side length.

A possible expansion of the study method presented may include taking into account the effect of the PCM thermal conductivity in order to achieve increased prediction accuracy and the ability to optimize the PCM performance towards protection time maximization. Furthermore, the introduction of electronics reliability dependence on

Published as: Kiziroglou and Yeatman, Journal of Electronic Materials, 44, 4589-4594, 2015

temperature would be of particular interest for ensuring reliable long-term operation. Such a consideration is expected to shift the optimal point, to guarantee a low-enough temperature during regular (i.e. non-harsh) operation for suitable reliability values. Finally, the combination of the proposed technique with state-of-the-art heat sinking technology such as heat pumping [16] should be studied, as it could lead to packaging solutions of increased performance in terms of protection duration and temperature limits.

The analytical model introduced in this paper allows a convenient and simple evaluation of the suitability of PCM encapsulation for different applications. This technique could contribute to enabling the use of electronics in transient harsh environments. The expected cost of adopting the proposed encapsulation technique is similar to any other PCM based thermal management solutions, because the materials used are commercially available at high volumes. Possible applications include sensor probing and industrial electronic installations involving time cycling operation.

REFERENCES

[1] R. Kandasamy, X.-Q. Wang, and A. S. Mujumdar, "Application of phase change materials in thermal management of electronics," *Applied Thermal Engineering,* vol. 27, pp. 2822-2832, 2007.

[2] R. Kandasamy, X.-Q. Wang, and A. S. Mujumdar, "Transient cooling of electronics using phase change material (PCM)-based heat sinks," *Applied Thermal Engineering,* vol. 28, pp. 1047-1057, 2008.

[3] R. Baby and C. Balaji, "Thermal performance of a PCM heat sink under different heat loads: An experimental study," *International Journal of Thermal Sciences,* vol. 79, pp. 240-249, 2014.

[4] S. C. Fok, W. Shen, and F. L. Tan, "Cooling of portable hand-held electronic devices using phase change materials in finned heat sinks," *International Journal of Thermal Sciences,* vol. 49, pp. 109-117, 2010.

[5] A. Hasan, S. J. McCormack, M. J. Huang, and B. Norton, "Evaluation of phase change materials for thermal regulation enhancement of building integrated photovoltaics," *Solar Energy,* vol. 84, pp. 1601-1612, 2010.

[6] J. Leland and G. Recktenwald, "Optimization of a phase change heat sink for extreme environments," in *Semiconductor Thermal Measurement and Management Symposium, 2003. Ninteenth Annual IEEE*, 2003, pp. 351-356.

[7] A. Alrashdan, A. T. Mayyas, and S. Al-Hallaj, "Thermo-mechanical behaviors of the expanded graphite-phase change material matrix used for thermal management of Li-ion battery packs," *Journal of Materials Processing Technology,* vol. 210, pp. 174-179, 2010.

[8] X. Duan and G. F. Naterer, "Heat transfer in phase change materials for thermal management of electric vehicle battery modules," *International Journal of Heat and Mass Transfer,* vol. 53, pp. 5176-5182, 2010.

[9] Z. Rao and S. Wang, "A review of power battery thermal energy management," *Renewable and Sustainable Energy Reviews,* vol. 15, pp. 4554-4571, 2011.

[10] Z. Ling, Z. Zhang, G. Shi, X. Fang, L. Wang, X. Gao, *et al.*, "Review on thermal management systems using phase change materials for electronic components, Li-ion batteries and photovoltaic modules," *Renewable and Sustainable Energy Reviews,* vol. 31, pp. 427-438, 2014.

[11] M. K. Rathod and J. Banerjee, "Thermal stability of phase change materials used in latent heat energy storage systems: A review," *Renewable and Sustainable Energy Reviews,* vol. 18, pp. 246-258, 2013.

[12] D. Smith, "An introduction to MSP430™ microcontroller-based temperature-sensing solutions," *Texas Instruments Technical White Paper,* 2013.

[13] PlusICE, "PlusICE Phase Change Materials," PCM Products Limited2014.

[14] M. Kiziroglou, A. Elefsiniotis, S. Wright, T. Toh, P. Mitcheson, T. Becker*, et al.*, "Performance of phase change materials for heat storage thermoelectric harvesting," *Applied Physics Letters,* vol. 103, p. 193902, 2013.

[15] S. Mahmoud, R. Al-Dadah, D. K. Aspinwall, S. L. Soo, and H. Hemida, "Effect of micro fin geometry on natural convection heat transfer of horizontal microstructures," *Applied Thermal Engineering,* vol. 31, pp. 627-633, 4// 2011.

[16] A. Sinha and Y. Joshi, "Performance of two-step thermoelectric-adsorption heat pump for harsh environment electronics cooling," in *Thermal and Thermomechanical Phenomena in Electronic Systems (ITherm), 2010 12th IEEE Intersociety Conference on*, 2010, pp. 1-9.

Published as: Kiziroglou and Yeatman, Journal of Electronic Materials, 44, 4589-4594, 2015